Molecular Dynamics Simulations of a Fluid Bilayer of Dipalmitoylphosphatidylcholine at Full Hydration, Constant Pressure, and Constant Temperature

Oliver Berger,* Olle Edholm,# and Fritz Jähnig*

*Max-Planck-Institut für Biologie, Abteilung Membranbiochemie, D-72076 Tübingen, Germany, and #Royal Institute of Technology, Department of Theoretical Physics, S-10044 Stockholm, Sweden

ABSTRACT   Molecular dynamics simulations of 500 ps were performed on a system consisting of a bilayer of 64 molecules of the lipid dipalmitoylphosphatidylcholine and 23 water molecules per lipid at an isotropic pressure of 1 atm and 50°C. Special attention was devoted to reproduce the correct density of the lipid, because this quantity is known experimentally with a precision better than 1%. For this purpose, the Lennard-Jones parameters of the hydrocarbon chains were adjusted by simulating a system consisting of 128 pentadecane molecules and varying the Lennard-Jones parameters until the experimental density and heat of vaporization were obtained. With these parameters the lipid density resulted in perfect agreement with the experimental density. The orientational order parameter of the hydrocarbon chains agreed perfectly well with the experimental values, which, because of its correlation with the area per lipid, makes it possible to give a proper estimate of the area per lipid of 0.61 ± 0.01 nm^2.

INTRODUCTION

In the past few years, a large number of molecular dynamics simulations of lipid bilayers have been reported. They varied in different respects, which can be grouped into different macroscopic boundary conditions (different ensembles) and different microscopic interaction parameters (force fields). In addition, more technical parameters, such as cutoffs in the microscopic interactions or step size and time window of the simulations, may vary.

Three different ensembles have been applied: constant volume (NVT) (Raghavan et al., 1992; Venable et al., 1993; Bassolino-Klimas et al., 1993; Heller et al., 1993; Essex et al., 1994; Robinson et al., 1994; Damodaran and Merz, 1994; Zhou and Schulten, 1995), constant surface tension equivalent to a constant anisotropic pressure (NγT) (Chiu et al., 1995; Feller et al., 1995), and constant isotropic pressure (NPT) (Egberts et al., 1994; Huang et al., 1994; Tu et al., 1995; Shinoda et al., 1995; Tieleman and Berendsen, 1996). Actually, constant volume means to keep the dimensions of a box constant, which is the standard condition to simulate a protein in a crystal lattice. This condition is not suitable, however, for a lipid bilayer, because the dimensions of the box are determined by the area and the length per lipid, which are not well known. Therefore, constant pressure is more suitable. The pressure may, however, be anisotropic. The symmetry of the surface and the condition of mechanical equilibrium leads to a diagonal pressure tensor with a constant normal pressure P_N that is equal to the external pressure (1 atm) and a pressure P_T in the two transverse

directions, which may depend upon the depth in the bilayer (z). The surface tension (γ) is defined by the relation $\delta W = \gamma dA$, where δW is the work required to change the surface area by dA. This means that the surface tension is equal to the derivative of the free energy with respect to area at constant temperature and volume:

$$\gamma = \left(\frac{\partial F}{\partial A}\right)_{T,V}. \tag{1}$$

Equivalently, one may calculate the work required to change the shape of a piece of bilayer at constant volume against a normal pressure P_N and a lateral pressure $P_T(z)$. If this is set equal to γdA, one obtains

$$\gamma = \int (P_N - P_T(z))\, dz, \tag{2}$$

where the integration is performed over the bilayer (see, e.g., Rowlinson and Widom, 1982, and Landau and Lifschitz, 1938, for a discussion and derivation of these results, which are general for a two-phase system with this symmetry). If the surface area can be fixed by external restraints as for Langmuir monolayers, the transverse pressure or the surface tension may be controlled and given a desired value. However, lipid bilayers are free to adjust their surface area to attain equilibrium with the surroundings. For a system at constant temperature and volume, other parameters will take on such values that the free energy is minimal (see any thermodynamics textbook). Thus the area will adjust so that the free energy becomes minimal.

For a mixture of two fluids with positive surface tension (like oil and water), the free energy increases monotonously with area. Thus the system tries to minimize the contact area (at constant volume). This gives rise to spherical drops of

one fluid in the other. If the surface tension is negative, the two fluids mix and there is no phase separation.

The situation is, however, more complicated for lipid bilayers. The hydrophobic effect, as for oil and water, will give rise to an increase in free energy with surface area. If this were all there is to consider, a bilayer would minimize its area at all temperatures and go into the ordered gel phase. This is obviously not what is observed in reality. The reason for this is that there are other contributions to the free energy that increase with decreasing surface area. A main source of this is that a small surface area will force the chains into a more ordered state and thus reduce the entropy of the system. This results in a free energy that no longer increases monotonously with area but has a minimum. The bilayer then adjusts its area to attain this minimum in thermodynamic equilibrium. This implies per definition that the surface tension is zero and the average transverse pressure is equal to the external pressure, as claimed by Jähnig (1996) in response to Chiu et al. (1995). The appropriate boundary condition for lipid bilayer simulations is therefore constant isotropic pressure (NPT).

The number of different force fields is even larger than the number of boundary conditions. Besides the packages such as AMBER (Weiner et al., 1984), CHARMM (Brooks et al., 1983), GROMOS (van Gunsteren and Berendsen, 1987), etc., special force fields have been introduced. Examples are the optimized parameters for liquid systems (OPLS) set of interaction parameters (Jorgensen and Tirado-Rives, 1988) and the Ryckaert-Bellemans model for hydrocarbon chains (Ryckaert and Bellemans, 1975, 1978). Another distinction refers to an all-atom description (Alper et al., 1993a; Bassolino-Klimas et al., 1993; Venable et al., 1993; Feller et al., 1995; Tu et al., 1995) or a unified description of CH_n groups, which may be further separated into the united atom (Raghavan et al., 1992; Heller et al., 1993; Marrink et al., 1993; Egberts et al., 1994; Essex et al., 1994; Huang et al., 1994; Robinson et al., 1994; Chiu et al., 1995; Shinoda et al., 1995; Zhou and Schulten, 1995; Tieleman and Berendsen, 1996) or the anisotropic united atom (Toxvaerd, 1990; Peters et al., 1994) model. Polarizable atoms are usually given fractional charges, which also may differ in their values. Different water models have also been used (Tieleman and Berendsen, 1996).

The results obtained under different conditions generally agree well with the available experimental data. A comparison is usually made for the area per lipid molecule, for the distances between certain atoms across the membrane, and for the orientational order parameter of the hydrocarbon chains. The order parameter was determined experimentally with an error of less than 1% (Seelig and Seelig, 1974), distances across the membrane with an error of ~5% (Büldt et al., 1979), whereas values for the area per lipid range from 0.56 nm² to 0.72 nm² (for a review see Nagle, 1993). Nagle (1993) has derived a relation between the order parameter and the area per lipid and concluded that 0.62 ± 0.02 nm² is the correct value for the lipid area, but the goodness of the approximations introduced in deriving the

relation was not tested. Hence there is a broad range of areas per lipid within which the result of simulations may be considered as acceptable. This excludes the area per lipid as a quantity that can be used for control of the quality of simulations and leaves the distances between certain atoms and the order parameter as useful quantities.

That so many simulations performed under different conditions arrive at similar results is a consequence of favorable combinations of parameters. Up to now, only a few studies were devoted to a systematic comparison of different parameters. Recently, Tieleman and Berendsen (1996) compared the three different ensembles (NVT, NγT, and NPT), two different water models, and two different sets of Lennard-Jones parameters between water and CH_n groups. They found that an NVT ensemble bears many problems and may lead to erroneous results, whereas NγT and NPT ensembles lead to similar results. Furthermore, SPC water seems to be generally better than SPC/E water when simulating interfaces, and a simple set of Lennard-Jones parameters between water and CH_n groups (van Buuren et al., 1993) is preferable over a more complex set.

Surprisingly, the density of the lipids or, equivalently, the volume per lipid has not received much attention in the analysis of simulations, although its value is known experimentally with an accuracy of less than 1% (Rand and Parsegian, 1989). Even more intriguing is the fact that in many simulations the volume per lipid deviates from the experimental value by more than 10%. If, however, the volume is not correct, it is unlikely that the area per lipid and the order parameter will be correct.

When we started our work, we were bothered by the fact that with the common force fields the volume per lipid turned out wrong. We obtained the best result with the OPLS force field developed by Jorgensen and Tirado-Rives (1988). The authors had already mentioned, however, that when using their parameters and going to higher homologs of the alkanes, the volume might become too low and the heat of vaporization too high (Jorgensen et al., 1984). Therefore it seemed reasonable to make the Lennard-Jones parameters for the CH_n groups responsible for the too low volume in the lipid simulations. To improve this deficiency, we simulated a system of pentadecane molecules, which should represent the hydrophobic chains of the lipids, and adjusted the Lennard-Jones parameters to yield the correct volume and heat of vaporization. With these parameters we simulated a bilayer of 64 molecules of dipalmitoylphosphatidylcholine and 23 water molecules per lipid for 500 ps. A constant isotropic pressure of 1 atm and a temperature of 50°C were applied, corresponding to an NPT ensemble. We compared three slightly different force fields. In simulation I we used the fractional charges of Essex et al. (1994), and in simulations II and III those derived by Chiu et al. (1995) (see also Tieleman and Berendsen, 1996). In simulations I and III the lipid headgroup was split up into two charged charge groups, one representing the choline moiety with a net charge of +1, the other the phosphate moiety with a net charge of −1. In simulation II the lipid headgroup was

treated as one large neutral charge group according to the method of Chiu et al. (1995). The quality of the simulations was tested by comparing the results for the volume per lipid, the distances between various atom pairs across the membrane, and the orientational order parameter of the lipid chains with the corresponding experimental data.

METHODS

Initial structure

Our system consists of 64 DPPC molecules located in the two halves of a planar bilayer and surrounded by a total of 1472 water molecules on both sides of the bilayer. This corresponds to 23 water molecules per lipid, which is within the range found experimentally for the number of water molecules at saturation (Nagle and Wiener, 1988). A control simulation with 40 water molecules per lipid was performed and did not exhibit any significant alteration.

The molecules were put into a rectangular box, with the xy plane defining the membrane plane and the z direction the membrane normal. The edge sizes of the box were fixed by assuming an initial value for the area per lipid of 0.65 nm^2, leading to $L_x = L_y = 4.56$ nm. This initial value for the area per lipid is higher than the expected value of 0.62 nm^2 (Nagle, 1993) and was chosen to give the system some flexibility in equilibration. For the volume per lipid, we assumed an initial value of 1.28 nm^3, which again is higher than the expected value of 1.23 nm^3. Together with a volume per water molecule of 0.03 nm^3, this leads to $L_z = 6.06$ nm.

The chemical formula of a DPPC molecule together with the numbering of atoms used is shown in Fig. 1. A three-dimensional structure of such a molecule was constructed by hand and was equilibrated by energy minimization and a short MD run. Twenty different equilibrated structures were gathered in a conformer library.

To put 64 lipid molecules into the initial box, a program SETLIP was written that places lipid molecules of the conformer library in a box. The different conformers are treated by SETLIP like rigid rods, with the long axis defined as the average of the two vectors along the two hydrocarbon chains. The carbon atom in the middle of the glycerol backbone (number 13 in Fig. 1) was chosen as the reference atom to position the lipid molecules randomly in the membrane plane, whereas the z coordinate of the reference atom was put in one of two layers separated by 3 nm with a spread of ± 0.3 nm around the mean values. Then there is an average distance between the phosphates at the two sides of the bilayer of 3.6 nm, which is within the range of experimentally determined values (Lewis and Engelman, 1983). The rods were rotated about their long axes to exclude a uniform orientation of the dipoles of the lipid headgroups. Finally, the rods were rotated about their short axes such that the orientation of their long axis varied within $\pm 30°$ around the membrane normal. The structure obtained was subjected to 500 steps of energy minimization to relax local stresses.

The remaining free space in the box was filled with water, using the GROMOS routine PROBOX, which uses as a building block a cubic box of 216 equilibrated water molecules. The minimum distance of water to lipid molecules was chosen as 0.18 nm. All water molecules that were placed inside the hydrocarbon core of 3.2 nm thickness were removed. The hydrated lipid bilayer was again subjected to 1000 steps of energy minimization.

Force field

For all bonds, valence angles, and improper dihedrals, as well as for the dihedral angles in the headgroup region, the standard parameters of the GROMOS force field were used. For the hydrocarbon chains the Ryckaert-Bellemans potential (Ryckaert and Bellemans, 1975, 1978) was used. For more details about the parametrization, see Egberts et al. (1994). The
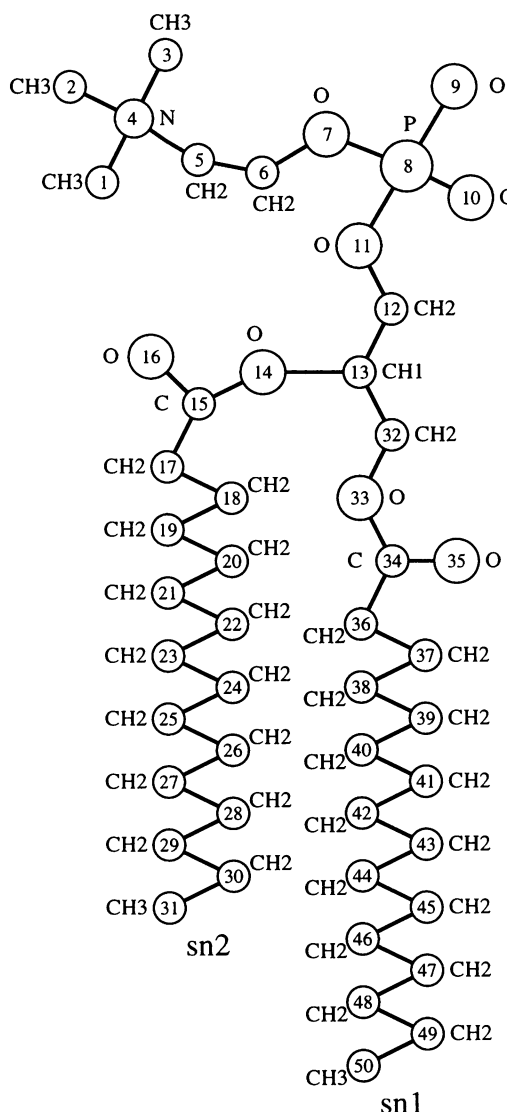

FIGURE 1 Chemical formula for dipalmitoylphosphatidylcholine (DPPC) with the numbering of the atoms as used in the simulations.

nonbonded interactions were computed according to the formula

$$V = \sum_{i>j}^{N} 4\epsilon \left[\left(\frac{\sigma_{ij}}{r_{ij}} \right)^{12} - \left(\frac{\sigma_{ij}}{r_{ij}} \right)^{6} \right] + \frac{1}{4\pi\epsilon_0} \frac{q_i q_j}{r_{ij}}, \qquad (3)$$

with the first term representing the Lennard-Jones interactions and the second term the Coulomb interactions. For the Lennard-Jones interactions, the OPLS parameters were applied (Jorgensen and Tirado-Rives, 1988), as also used by Essex et al. (1994). During our studies, the interaction parameters for the united CH$_n$ groups of the lipid chains were adjusted by reference to pentadecane, as will be described. The Lennard-Jones parameters used are listed in Table 1. The combining rules to get the mixed Lennard-Jones parameters were those implemented in the GROMOS force field, namely the geometric mean for the ϵ and σ values. For the nonbonded 1,4 interaction, the Lennard-Jones contribution was reduced by a factor of 8, as recommended for the OPLS parameter set (Jorgensen and Tirado-Rives, 1988).

For the electrostatic interactions, the fractional charges suggested by Essex et al. (1994) based on the OPLS charges were used in simulation I. Because these were derived by the questionable transfer of charges from

TABLE 1   Lennard-Jones parameters σ and ε and fractional charges q for lipid and water

n	Name	σ (nm)	ε (kJ/mol)	q Sim I	Sim II, III
1–3	Cγ	0.396	0.606	0.25	0.40
4	N	0.325	0.711	0.00	−0.50
5	Cβ	0.3905	0.606	0.25	0.30
6	Cα	0.380	0.606	0.20	0.40
7		0.300	0.711	−0.43	−0.80
8	P	0.374	0.836	0.78	1.70
9–10		0.296	0.878	−0.66	−0.80
11		0.300	0.711	−0.43	−0.70
12	GC3	0.380	0.606	0.20	0.40
13		0.380	0.334	0.25	0.30
14		0.300	0.711	−0.40	−0.70
15	C1sn1	0.375	0.438	0.55	0.70
16		0.296	0.606	−0.45	−0.70
17	C2sn2	0.396	0.380	0.05	0.00
18–30	C3–C15sn2	0.396	0.380	0.00	0.00
31	C16sn2	0.396	0.570	0.00	0.00
32		0.380	0.606	0.25	0.50
33		0.300	0.711	−0.40	−0.70
34	C1sn1	0.375	0.438	0.55	0.80
35		0.296	0.606	−0.45	−0.60
36	C2sn1	0.396	0.380	0.05	0.00
37–49	C3–C15sn1	0.396	0.380	0.00	0.00
50	C16sn1	0.396	0.570	0.00	0.00
	OW	0.317	0.650	−0.82	−0.82
	HW	0.000	0.000	0.41	0.41

Numbers n agree with the numbers in Fig. 1.

smaller molecules, we tested another set of fractional charges in simulation II and III, those of Chiu et al. (1995). These charges come from an ab initio quantum mechanical calculation which, as discussed by Essex et al. (1994), is not without difficulties for a molecule of this type. These are only two of several different charge distributions in the literature, and it remains unclear which one is the best. The fractional charges used are listed in Table 1. In simulation I the charge groups were built by atom number 1–5, 6–12, 13–17, and 32–36, with the former two groups bearing a net charge. In simulation II, the charge groups were those proposed by Chiu et al. (1995), namely built by atom number 1–11, 12–16, and 32–35, which are all neutral. In simulation III, the large charge group of simulation II, consisting of atom numbers 1–11, was cut in two pieces, one covering atom number 1–5, the other number 6–11. This implies that the charge groups now bear a net charge. The 1,4 electrostatic interaction was not scaled.

Water model

For water, we used the single point charge (SPC) model, as recommended by van Buuren et al. (1993), when simulating interfaces. For the interaction between water oxygen and other atoms, a unique set of parameters was used, and no distinction between hydrophobic and hydrophilic atoms was made. This is equivalent to the proposal made by Tieleman and Berendsen (1996), based on the results of van Buuren et al. (1993).

Simulation conditions

For all Lennard-Jones interactions, a cutoff of 1.0 nm was used. For the electrostatic interactions, a group-based twin-range cutoff was used in which the interactions of groups within a distance of 1 nm are calculated for every time step, and interactions of groups at a distance between 1 and 1.8 nm are stored in a pair list that is updated every 10 time steps.

Because of the hand-made nature of the initial structure, great care was devoted to the equilibration process. The equilibration of simulation I was performed in the following three steps.

1. The system was simulated at constant volume (NVT) to equilibrate the distribution of the atoms so that regions of high pressure vanish. The initial atomic velocities were taken from a Maxwell-Boltzmann distribution at 50°C. The time constant for coupling to the temperature bath was 10 fs, and the equilibration was extended over 10 ps. Bonds were kept constant by using the SHAKE algorithm.

2. After the first 10 ps the system was coupled to an isotropic pressure bath by scaling the three unit cell dimensions individually to 1 atm (NPT) with a time constant of 50 fs (Berendsen et al., 1984). The duration of this step was again 10 ps.

3. Finally, the strength of the coupling to the temperature and pressure bath was weakened by increasing the time constants by a factor of 10, i.e., to 100 fs for the temperature bath and 500 fs for the pressure bath.

For equilibration of simulations II and III, we started from a snapshot structure after 400 ps of simulation I. Three short equilibration steps were performed:

1. The NPT ensemble was simulated for 1000 steps with a step size of 0.5 fs and strong coupling to the temperature and pressure bath, i.e., time constants of 10 and 50 fs, respectively.

2. A simulation for 500 steps with a step size of 1 fs and strong coupling was performed.

3. Finally, a simulation for 500 steps with a step size of 2 fs and weak coupling was performed, i.e., time constants of 100 and 500 fs for the temperature and pressure bath, respectively.

After the equilibration process, the production runs were started. The conditions were the same as for the third equilibration step. The length of the production runs was 500 ps.

Cutoff correction

Because of the cutoff for calculating the intermolecular interactions, an error in the energy and volume is made. For a Lennard-Jones fluid an estimate of the error can be computed in the usual way according to

equations (4) and (5) (see Appendix for the derivation):

$$\Delta E = - \frac{8\pi N^2}{3V} \frac{\epsilon \sigma^6}{r_c^3} \qquad (4)$$

$$\Delta V = -\kappa \frac{16\pi N^2}{3V} \frac{\epsilon \sigma^6}{r_c^3}, \qquad (5)$$

where N is the number of monomers, ϵ and σ are the Lennard-Jones parameters, r_c is the cutoff radius, and κ is the isothermal compressibility.

Our system is more complicated because it also involves bonded interactions and electrostatic ones and has different Lennard-Jones parameters for different atoms. Still, because Lennard-Jones interactions dominate the cohesive forces of the system, an estimate of the small correction due to the finite cutoff using the equations above with the average Lennard-Jones parameters of the system makes sense. The long-range electrostatic interactions have been calculated up to a cutoff of 1.8 nm by using a twin-range update method, which is enough for a system like ours (Alper et al., 1993a,b). The contributions of the electrostatic interactions beyond the long-range cutoff have been shown to be negligible (Berendsen et al., 1992).

Optimization of Lennard-Jones parameters

For the optimization of the Lennard-Jones parameters, we constructed a system of 128 chains of pentadecane and performed simulations under a constant temperature of 50°C and a constant pressure of 1 atm. For comparison with experiment, the volume per pentadecane and the heat of vaporization were chosen. It turned out that a relatively short simulation length of 10 ps was sufficient to reach equilibrium of the quantities of interest. The volume follows directly from the size of the periodic simulation box, whereas the heat of vaporization ΔH_{vap} is calculated as usual from equation (6).

$$\Delta H_{vap} = E(\text{gas}) - E(\text{liquid}) + NkT. \qquad (6)$$

For the determination of E(gas) we performed a 1.28-ns vacuum simulation of one monomer of pentadecane at 50°C. The intermolecular interactions between monomers in the gas phase are neglected. E(liquid) is built up from intramolecular and intermolecular contributions (E(liquid) = E^{intra}(liquid) + E^{inter}(liquid)). The intermolecular energy was calculated under consideration of the cutoff correction (E^{inter}(liquid) = E_0^{inter}(liquid) + ΔE). The Lennard-Jones parameters for the interaction of CH_2 and CH_3 groups were varied in a systematic way until the volume per pentadecane and the heat of vaporization were obtained, such that after correcting for the cutoff, the experimental values were reproduced. This corresponds to the original procedure of Jorgensen et al. (1984). Because there are not enough experimental parameters to determine the Lennard-Jones parameters of the CH_3 groups independently, these were chosen as

$$\sigma_{CH_3} = \sigma_{CH_2} \quad \text{and} \quad \epsilon_{CH_3} = 3/2\epsilon_{CH_2}. \qquad (7)$$

The choice of ϵ means that we assume that the strength of the Lennard-Jones interactions is proportional to the number of C-H bonds. These choices are in agreement with many but not all other force fields (see Table 2).

RESULTS AND DISCUSSION

Pentadecane

When we started our simulations, we recognized that with common Lennard-Jones parameters for the interaction of CH_n atoms, the volume per lipid turned out to be wrong.

TABLE 2 Lennard-Jones parameters σ and ϵ of CH_2 and CH_3 groups of some force fields

Source	CH₂		CH₃	
	σ (nm)	ϵ (kJ/mol)	σ (nm)	ϵ (kJ/mol)
GROMOS*	0.396	0.585	0.379	0.753
Egberts[#]	0.375	0.430	0.375	0.625
OPLS[§]	0.3905	0.4932	0.3905	0.7315
Heller[¶]	0.398	0.477	0.386	0.757
PD[∥]	0.396	0.380	0.396	0.570

*ifp37C4 force field parameters.

[#]From Egberts et al. (1994).

[§]From Jorgensen and Tirado-Rives (1988).

[¶]From Heller et al. (1993), and Heller, personal communication.

[∥]Optimized parameters of the pentadecane simulation.

The volume per lipid (V_L) is calculated from the relation

$$V_{box} = N_L \times V_L + N_W \times V_W, \qquad (8)$$

using for the volume of water V_W the values determined from separate simulations of pure water under the appropriate conditions. We tested the GROMOS force field and the OPLS parameter set and obtained 1.075 nm³ and 1.190 nm³, respectively, for the volume per lipid; the experimental value was 1.232 nm³ (Nagle and Wiener, 1988). The OPLS value is close to the experimental value, but the cutoff correction (see Methods) reduces it further. Results from the literature support this conclusion. For example, in the simulations of Tieleman and Berendsen (1996), we obtained a volume of 1.080 ± 0.020 nm³ when using equation (8) with $V_W = 0.03$ nm³.

Jorgensen et al. (1984) had already suggested that the Lennard-Jones parameters for CH_n interactions might be wrong for hydrocarbon chains longer than hexane. Therefore, we constructed a system of 128 chains of pentadecane and tested some of the Lennard-Jones parameters commonly used for lipid simulations with respect to the volume per pentadecane and the heat of vaporization. With the original OPLS parameters (Jorgensen et al., 1984), the volume per pentadecane chain (V) was 0.434 nm³, and the heat of vaporization (ΔH_{vap}) was 86.0 kJ/mol, including the cutoff correction. The experimental values are 0.469 nm³ and 61.2 kJ/mol, respectively, with $\kappa = 0.97 \times 10^{-4}$ atm⁻¹ at 50°C for pentadecane (Handbook of Physics and Chemistry, 54th edition). Similar results have been obtained with Lennard-Jones parameters of other force fields, in that the volume was too small and the heat of vaporization too high. The Lennard-Jones parameters of other force fields that have been tested are listed in Table 2; the volume and the heat of vaporization obtained with these parameters in a pentadecane simulation are listed in Table 3.

The effect of increasing σ is a gain in volume, whereas decreasing ϵ results in a lowering of the heat of vaporization. The values for ϵ and σ obtained in a systematic optimization procedure implied a change in the original OPLS parameters ϵ and σ for the interaction of CH_2 groups from $\epsilon = 0.49$ kJ/mol and $\sigma = 0.391$ nm to $\epsilon = 0.38$ kJ/mol

TABLE 3   Volume and heat of vaporization of pentadecane obtained with Lennard-Jones parameters of the force fields listed in Table 2

Source[*]	ΔV (nm^3)	V (nm^3)	E(gas) (kJ/mol)	E^{intra}(liquid) (kJ/mol)	E_0^{inter}(liquid) (kJ/mol)	ΔE (kJ/mol)	ΔH_{vap} (kJ/mol)
GROMOS	−0.0072	0.417	38.7	47.1	−110.3	−2.2	106.8
Egberts	−0.0038	0.421	42.8	47.5	−67.6	−1.2	66.8
OPLS	−0.0054	0.434	40.7	47.0	−87.9	−1.7	86.0
Heller	−0.0057	0.443	40.6	47.0	−88.6	−1.8	86.7
PD	−0.0041	0.473	41.3	46.9	−63.4	−1.3	61.8
Exp		0.469[#]					61.2[#]

[*]See Table 2 for the different sources of the force fields.
[#]*Handbook of Physics and Chemistry*, 54th edition.
The standard error of the simulated volume amounts to less than 0.003 nm^3, and that of the energies to less than 0.4 kJ/mol.

and $\sigma = 0.396$ nm, respectively, and similar changes for the interaction of CH_3 groups according to equation (7).

Comparison of the optimized parameters with standard values of Table 2 shows that σ is in the middle of the range of the usually applied values, whereas ϵ is even 12% lower than the smallest value. This means that the main changes have been performed on ϵ, and not on σ, which would have been the obvious change for adjusting the volume. The lowering of ϵ for the hydrocarbons in a lipid simulation could have a destabilizing effect on the bilayer by decreasing the interaction of the hydrocarbon chains and therefore a lowering of the phase transition temperature in comparison to higher values of ϵ. This could shed light on the problems of other groups that obtained a gel phase with the standard parameters but otherwise similar conditions (Egberts et al., 1994). They solved their problems by reducing the charges to reduce the attractive forces in the system.

Lipid bilayer

A planar bilayer of 64 DPPC molecules and 23 water molecules per lipid was simulated at a constant temperature of 50°C and a constant pressure of 1 atm (NPT). The Lennard-Jones parameters for the interaction of CH_n groups as adjusted for pentadecane were used. Three kinds of simulations were performed. In simulation I, the fractional charges of Essex et al. (1994) were used; in simulations II and III, those of Chiu et al. (1995) were used. In simulations I and III the lipid headgroup was split into two charge groups, whereas in simulation II the lipid headgroup was treated as a large neutral charge group according to the method of Chiu et al. (1995). A picture of the structure after 500 ps of simulation I is shown in Fig. 2. Obviously, the lipid chains are in the fluid state, the lipid headgroups exhibit a broad distribution of their positions along the membrane normal, and water is penetrating deep into the headgroup region, as reported already in the literature (Marrink et al., 1993).

The time courses of the volume per lipid, the area per lipid, and the bilayer repeat distance are shown in Fig. 3 for the three simulations. The area per lipid and the bilayer repeat distance equilibrate after ~200 ps. This is also true for the potential energy (data not shown) and is in accord
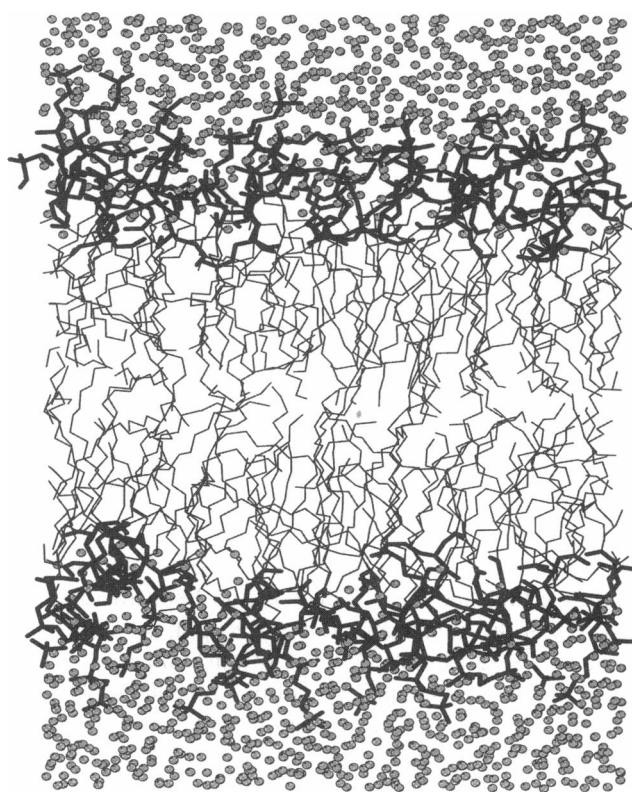

FIGURE 2   Side view of the structure of the bilayer system after 500 ps of simulation I. Bold lines are used for the headgroup and the glycerol moiety of the lipids, thin lines for the hydrocarbon chains, and grey spheres for the water molecules.

with the results of Tu et al. (1995), who performed a long NPT simulation of 1.5 ns. Therefore, only the last 300 ps of the production runs was used for the analysis of the trajectories.

The mean values over the last 300 ps for the volume per lipid, the area per lipid, and the bilayer repeat distance are listed in Table 4. The values for the volume per lipid differ only slightly for the different simulations, and all agree with the experimental value within 1%. However, as for pentadecane, we must take into consideration a volume correction. For calculating the volume correction of DPPC we used equation (5), bearing in mind that this can only be a
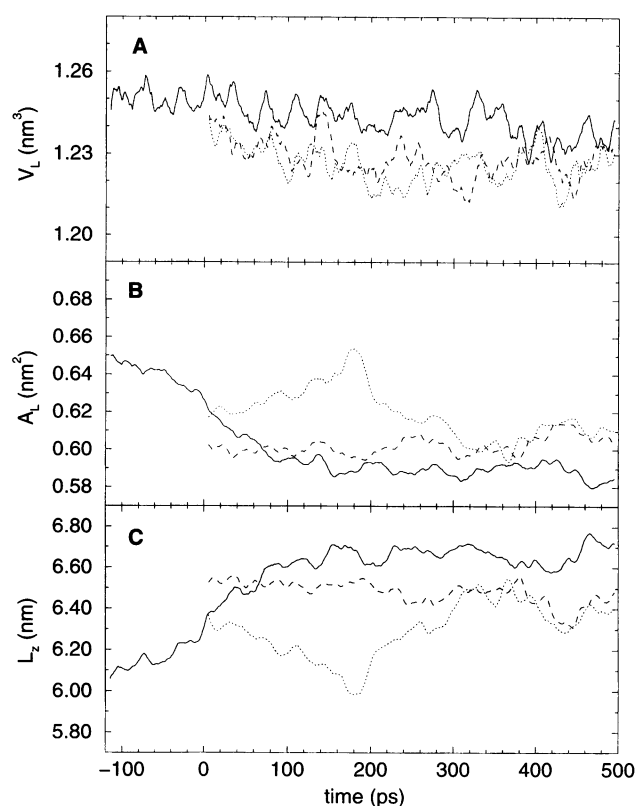
FIGURE 3 Temporal evolution of the volume per lipid V_L (*A*), the area per lipid A_L (*B*), and the bilayer repeat distance L_Z (*C*) for simulation I (——), II (·····), and III (– – –).

crude approximation, because DPPC is not a Lennard-Jones fluid. We took the mean values of the Lennard-Jones parameters of the atoms comprising the lipid, $\sigma = 0.376$ nm and $\epsilon = 0.492$ kJ/mol, $V = 1.232$ nm^3 and $N = 50$. To determine the compressibility κ of the simulated system, we performed two additional simulations with cutoffs of 1.5 nm and 1.8 nm and yielded a value of $\kappa = 4.5 \times 10^{-5}$ atm^{-1} using equation (5). With these values the volume correction amounts to $\Delta V = 0.035$ nm^3, i.e., 2.9% of the total volume when using a cutoff of 1.0 nm. That means after inclusion of the volume correction we obtained volumes of 1.205 nm^3, 1.189 nm^3, and 1.191 nm^3 for simulations I, II, and III, respectively. These lipid volumes are too small but do not deviate by more than 3.5% from the experimental value, and therefore the error is acceptable. A further improvement in adjusting the correct volume could be reached by also optimizing the Lennard-Jones parameters of the lipid headgroups.

The area per lipid is relatively small for simulation I; for the other two simulations the numbers lie within 3% of the value 0.62 nm^2, which is generally considered the best experimental value (Nagle, 1993). For simulation II, the area per lipid varies most strongly. This might be due to the large charge groups used in this simulation, in combination with the center of mass criterion for updating the molecular pair list. Moreover, the local headgroup interaction became

more anisotropic, which explains the observed development of an asymmetry in the x and y dimensions of 4.9 nm and 4.0 nm, respectively, in the course of the first 200 ps of the simulation. This was the reason for us to diminish the charge groups in simulation III, where, as well as in simulation I, no asymmetry was observed.

Included in Table 4 are the mean distances between pairs of atoms on both sides of the bilayer, e.g., of Cβ atoms in the headgroup region and of C9 atoms in the chain region. The three simulations differ slightly in the results with a deviation of about 3%, simulation II usually providing the lowest value for the distances, which agrees best with the experimental results. Actually, the atoms are spread out over quite large regions, as can be seen from Fig. 4, where the densities of different atoms or groups of atoms are plotted. The phosphate and the choline groups as well as the carbonyl groups have a spread of about 1 nm. The CH$_3$ groups at the end of the chains are even more smeared out and cover a range of about 2 nm in the middle of the bilayer. Included in Fig. 4 is the variation in the total densities of lipid and water. The decrease in the lipid density in the middle of the bilayer by a factor of about 1/2 is in agreement with the experimental results (Franks, 1977). Water enters the bilayer down to the carbonyl groups, leaving a region of only 2 nm devoid of water. Similar results have already been reported in the literature (Egberts et al., 1994).

The variation of the orientational order parameter along the hydrocarbon chains of the lipids is shown in Fig. 5. The results for the three simulations differ slightly, but all show the typical variation, with a plateau over the central region of the chains and a decrease toward the chain ends. The average deviation from the experimental values for simulations I, II, and III is 0.0093, 0.0045, and 0.0144, i.e., 5.5%, 2.7%, and 8.4%, respectively. Simulation I yields the highest order parameter in the central region, whereas in the end region the values for simulation III are higher. The results from simulation II agree perfectly well with the experimental values, which lie well within the standard deviation of the simulated values calculated as averages over successive 50 ps, except for carbon atom number 3, which shows the largest deviation.

It seems intuitively clear that the ordering of the chains should decrease with increasing area per lipid. Because our system is simulated at constant pressure and is fairly small, there are substantial fluctuations in surface area during the simulations. The average area per lipid in successive 50-ps parts of the simulation fluctuates between 58 and 64 Å^2. The average order parameter, corresponding to the deuterium order parameter, over the plateau region was then calculated separately over these 50-ps parts and is shown in Fig. 6 versus area per lipid. Different relations between this order parameter and the area per lipid have been suggested in the literature. In Fig. 6 we also show a line based on an approximate theoretical model (Nagle, 1993). This line fits the data reasonably well, but is clearly somewhat too steep. If simulation II (*circles*) is taken into account, which we consider the best simulation, the agreement is better (data

TABLE 4 Mean values of the volume per lipid V_L, the area per lipid A_L, the bilayer repeat distance L_z, and the distances of certain pairs of atoms across the bilayer for simulations I, II, and III, averaged over the last 300 ps of the production runs

	Sim I	Sim II	Sim III	Exp
V_L (nm^3)*	1.240 (0.008)	1.224 (0.009)	1.226 (0.008)	1.232 (0.012)[§]
A_L (nm^2)#	0.589 (0.004)	0.611 (0.008)	0.604 (0.005)	0.62 (0.02)[¶]
L_z (nm)	6.67 (0.05)	6.37 (0.09)	6.45 (0.06)	6.22 (0.25)
Cβ–Cβ (nm)	4.30 (0.44)	4.12 (0.49)	4.15 (0.55)	4.24 (0.2)[∥]
GC3–GC3 (nm)	3.67 (0.34)	3.55 (0.34)	3.60 (0.46)	3.48 (0.3)[∥]
C4–C4 (nm)	2.55 (0.39)	2.47 (0.40)	2.51 (0.48)	2.44 (0.3)[∥]
C9–C9 (nm)	1.60 (0.43)	1.54 (0.42)	1.57 (0.49)	1.61 (0.2)[∥]
C14–C14 (nm)	0.76 (0.51)	0.72 (0.46)	0.73 (0.52)	0.72 (0.2)[∥]

*The volume per lipid is calculated from the relation $V_{box} = N_L \times V_L + N_W \times V_W$, using for the volume of water the value 0.0314 nm^3, which was determined from a separate simulation of pure water.
#The area per lipid was calculated from the relation $L_x \times L_y = 1/2N_L \times A_L$.
§From Nagle and Wiener (1988).
¶From Nagle (1993).
∥From Büldt et al. (1979).
The figures in parentheses represent the standard deviation. For comparison, the experimental values are included.

not shown), but the line of Nagle is still somewhat too steep, and the absolute values of his order parameters slightly too large. If the order parameters all along the chain are included in the averaging, the agreement would clearly be worse, but this should also be expected, because the model neglects upturns, which contribute more in the tail region.

The experimental NMR order parameter, averaged over the plateau region, becomes -0.206, when the data of Seelig and Seelig (1974) are used. If an area per lipid corresponding to this order parameter is read off from the fitted straight line in Fig. 6, we get the area 0.61 nm^2. This is consistent with the actual area obtained in the simulation. Chiu et al. (1995) obtain 0.62 nm^2 by such a procedure, whereas the actual area in their simulation is 0.572 nm^2. The reason for this difference is that their volume per lipid is 12% too small.

In Fig. 7, two order parameters are shown against each other,

$$\langle P_1 \rangle = \langle \cos \theta \rangle \quad \text{and} \quad \langle P_2 \rangle = (3\langle \cos^2\theta \rangle - 1)/2, \quad (9)$$

where θ is the angle between the membrane normal and the vector joining the nearest-neighbor carbons on each side of the carbon hydrocarbon group for which we define the order parameter. The order parameter $\langle P_2 \rangle$ is approximately related to the order parameter S_{CD} as $\langle P_2 \rangle = -2S_{CD}$. The dots are averages over time but not over the chain positions for the three simulations. The points at the right with small values on both order parameters correspond to the tails of the chains. The order parameter $\langle P_1 \rangle$ is proportional to the
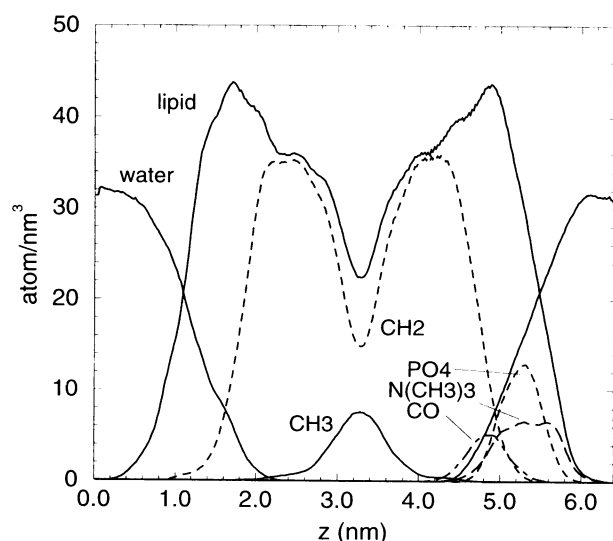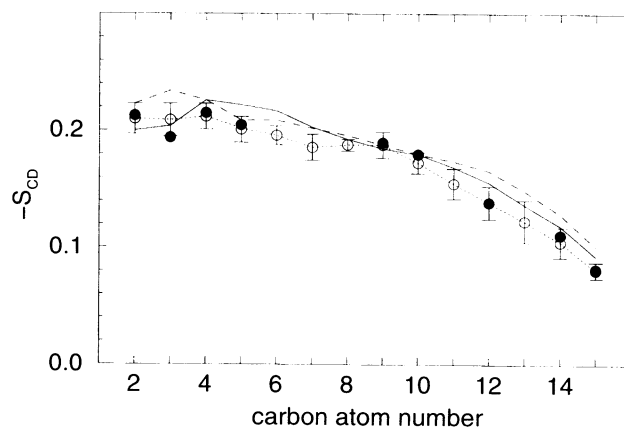

FIGURE 4 Profiles across the bilayer of the total lipid density, the water density, and the densities of certain lipid groups. Mean values over 10 ps of the last 300 ps of simulation II are plotted. The densities for the lipid headgroup components are only shown on one side for clarity.

FIGURE 5 Variation of the orientational order parameter S_{CD} along the hydrocarbon chains of the lipids for simulation I (———), II (·····), and III (– – –). The orientational order parameter is calculated as the mean value of the second-order Legendre polynomial $P_2(\cos \theta) = (3 \cos^2\theta - 1)/2$ averaged over the last 300 ps and all chains. θ is the angle between the CD bond and the bilayer normal. The positions of the deuterium atoms were reconstructed from the coordinates of the acyl chain carbons C_{n-1}, C_n, and C_{n+1}, assuming ideal geometry of the CD bond. For comparison, the experimental values (●) are included (Seelig and Seelig, 1974). Error bars, which are only shown for simulation II (○), represent the standard deviation of averages over successive 50 ps.
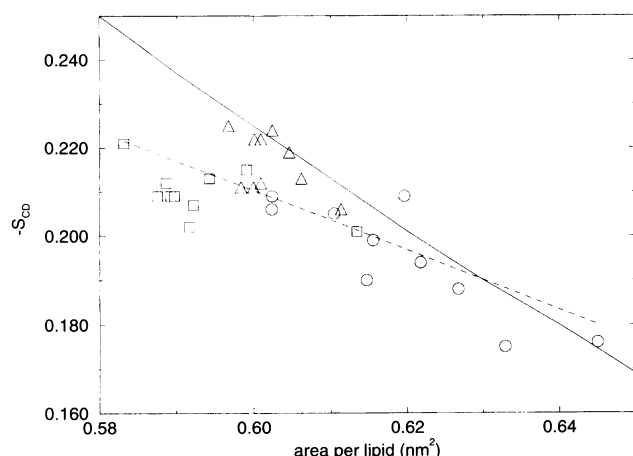
FIGURE 6 Dependence of the simulated order parameter S_{CD} averaged over the plateau region (hydrocarbons 2–8) on the area per lipid for successive 50-ps averages for simulation I ($\square$), II ($\bigcirc$), and III ($\triangle$). – – –, Least-square fit to the 30 points. ——, Model of Nagle (1993).

extension of a hydrocarbon group in the normal direction. Because the volume occupied by a hydrocarbon group is approximately constant, the order parameter is inversely proportional to the area per lipid, and therefore Fig. 7 looks similar to Fig. 6. The full line corresponds to the model by Nagle cited above. This line is clearly steeper than our data and overestimates $\langle P_2 \rangle$ on the left side (plateau region), whereas it underestimates $\langle P_2 \rangle$ on the right side (tail region). It is still much closer to our data than the model suggested by De Young and Dill (1988) (*top line*) that was based on a simple cubic lattice. We also show the lower limit on $\langle P_2 \rangle$ in the figure. This is obtained if $\langle \cos^2 \theta \rangle = \langle \cos \theta \rangle^2$, which would occur if the chains were tilted in the all-*trans* state. The distance to that line is a measure for the extent to which real disorder and not just a deterministic tilt contributes to order parameters different from 1. Clearly, our simulations show less real disorder in the high-order parameter end and
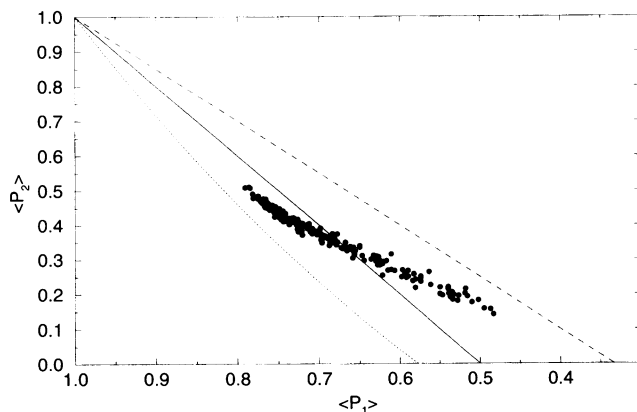

FIGURE 7 The order parameter $\langle P_2 \rangle$ versus $\langle P_1 \rangle$ for individual hydrocarbons averaged over time subsets of the three simulations. Also shown is the lower limit, where $\langle \cos^2 \theta \rangle = \langle \cos \theta \rangle^2$ ($\cdots$), the model of Nagle (——), and the model of De Young and Dill (– – –).

more real disorder in the low-order parameter end than the model of Nagle.

As a further result we present the variation of the electric potential across the bilayer in Fig. 8. From the separate contributions of the lipid and water atoms, it is obvious that the lipids provide a positive potential in the water layer and the water molecules provide a negative one, but such that in the sum the water dominates and the total potential is negative in the water layer. The three simulations exhibit significant differences in the total potential. For simulation I, the potential decreases monotonously to a value of about -740 mV in the center of the water layer. For simulations II and III, the potential first increases and then decreases to a value of -130 or -250 mV, respectively. This is in accord with results recently obtained by Tieleman and Berendsen (1996). It seems that the overall shape of the potential is dependent on the fractional charges used in the simulations and can thus be a valuable tool in judging the different partial charges if experimental results would favor one or the other shape. Experimental results for the electric potential are not fully conclusive, but differences between water and the bilayer interior of several 100 mV with the bilayer interior positive seem to have been observed (Gawrisch et al., 1992).

CONCLUSION

Our first aim was to simulate a lipid bilayer and obtain the correct lipid density, because if the density is not correct there seems to be no chance to get the area per lipid correct. This aim was reached by adjusting the parameters for the Lennard-Jones interaction between CH_n groups for pentadecane. When we adopted these parameters to simulate a lipid bilayer, the volume per lipid agreed within 1% of the experimental value of 1.232 nm^3. After inclusion of the cutoff correction, the volume was too small but still remained within 3% of the experimental value. All three simulations gave comparable results for the distances of certain pairs of atoms across the bilayer, which remained within 3% of the experimental values. The orientational order parameter for the lipid chains agreed best with the experimental values for simulation II, where the simulated values again are within 3% of the experimental ones.

The area per lipid was obtained as 0.61 nm^2 for simulation II. This agrees exactly with the area obtained from the relation between the order parameter and the area per lipid shown in Fig. 6 if the experimental order parameter value is inserted. This is close to the value of 0.62 nm^2, which is generally considered to be the correct value. This result may be compared to other united atom simulations. Tielman and Berendsen (1996) get 0.60 nm^2 with SPC water at isotropic pressure (and 0.61 nm^2 at a constant nonzero surface tension), whereas Chiu et al. (1995) obtain 0.572 nm^2 in their study. In the all-atom model simulations by Tu et al. (1995), the area is 0.618 nm^2, whereas it is 0.65 nm^2 in the case of Feller et al. (1995).

FIGURE 8   Variation of the electric potential Ψ across the bilayer. In A, the lipid (*upper curve*) and water (*lower curve*) contributions are plotted separately for simulation I. In B, the total potential is plotted for simulation I (——), II (·····), and III (– – –). The electric potential is calculated by double integration of the charge density. Note that the z coordinate is shifted; zero corresponds to the water layer.
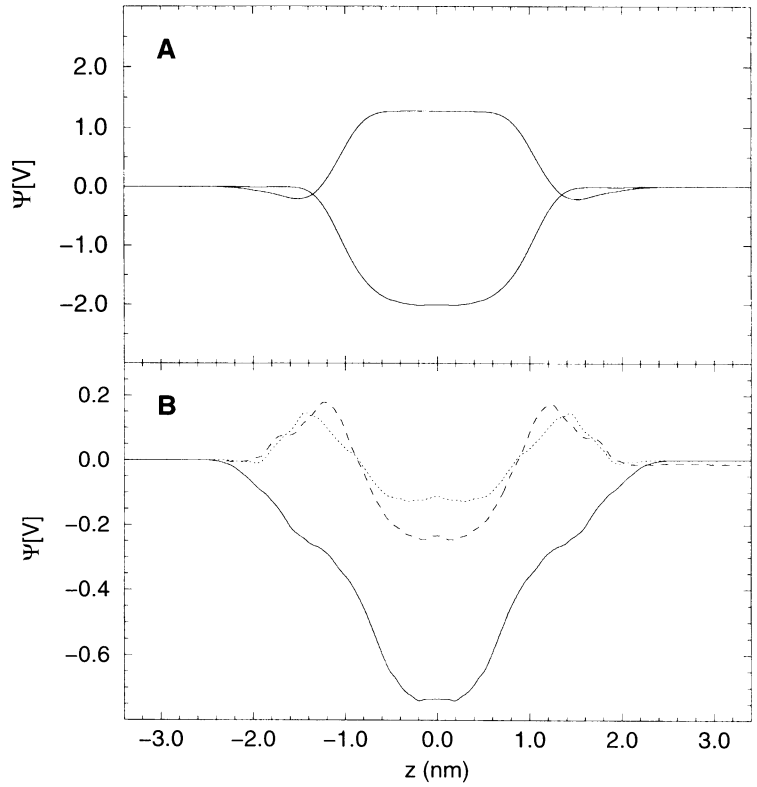
In summary this shows that some care is needed to describe the hydrocarbon part of the bilayer properly with a united atom model as well as with an all-atom model.

This and other simulations give a reasonable structure of the headgroup region. Still, the difference in the electric potential depending upon the choice of the fractional charges shows that results are sensitive to details in the force field, and more accurate experimental data are needed to validate a certain choice from a simulation.

APPENDIX: CUTOFF CORRECTION

An estimate can be given for the error made in the computation of the energy and the pressure when using a finite cutoff in simulations of a system consisting of Lennard-Jones particles (for reference see any textbook on statistical mechanics). The mean total interaction energy of N Lennard-Jones particles may be calculated as

$$E = \frac{1}{2}\left\langle \sum_{i,j}^{N} \Phi(r_{i,j}) \right\rangle, \tag{A.1}$$

with Φ denoting the Lennard-Jones interaction energy and the brackets the temporal average. The factor $\frac{1}{2}$ prevents double-counting of the interactions. Because, on average, all particles are equivalent, one sum can be replaced by a factor N:

$$E = \frac{N}{2}\left\langle \sum_{j}^{N} \Phi(r_{i,j}) \right\rangle. \tag{A.2}$$

The space around particle i may be split up into spherical shells, and the number density $\rho = N/V$ and the pair correlation function of the particles

$g(r)$ may be introduced. This leads to

$$E = \frac{N}{2}\int_{0}^{\infty} \Phi(r)\rho g(r)4\pi r^2 \, dr. \tag{A.3}$$

The integral may be divided into a region from zero to the cutoff radius r_c and a region from r_c to infinity. The first part yields the total interaction energy E_0, as calculated in the simulations, and the second part represents the correction due to the cutoff. In this part, which covers long distances, the repulsive term in the Lennard-Jones interaction $\Phi(r) = 4\epsilon[(\sigma/r)^{12} - (\sigma/r)^6]$ may be neglected, and the pair correlation function $g(r)$ may be taken to be 1, so that one obtains

$$E = E_0 - \frac{2\pi N^2}{V}\int_{r_c}^{\infty} 4\epsilon\left(\frac{\sigma}{r}\right)^6 r^2 \, dr, \tag{A.4}$$

and finally

$$E = E_0 - \frac{8\pi N^2}{3V}\frac{\epsilon\sigma^6}{r_c^3}. \tag{A.5}$$

The second term, $\Delta E = (-8\pi N^2/3V)(\epsilon\sigma^6/r_c^3)$, represents the cutoff correction for the energy.

In analogy to this procedure, the correction for the pressure P or the volume V may be estimated starting from the virial theorem

$$PV = NkT + \frac{1}{3}\left\langle \sum_{j}^{N} \mathbf{F}_j \cdot \mathbf{r}_j \right\rangle, \tag{A.6}$$

with $\mathbf{F}_j$ denoting the force acting on particle j at position $\mathbf{r}_j$ due to the presence of all other particles. For interactions that depend only on the

distance between the particles, such as Lennard-Jones interactions, the second term can easily be transformed into

$$PV = NkT + \frac{1}{6} \left\langle \sum_{i,j}^{N} F(r_{ij}) r_{ij} \right\rangle. \qquad (A.7)$$

Remembering that $F = -d\Phi/dr$, this expression resembles equation (A.1), and by the same procedure described above it can be written as

$$PV = NkT - \frac{N}{6} \int_{0}^{\infty} \frac{d\Phi}{dr} \rho g(r) 4\pi r^2 \, dr, \qquad (A.8)$$

which finally leads to

$$P = P_0 - \frac{16\pi N^2}{3V^2} \frac{\epsilon \sigma^6}{r_c^3}. \qquad (A.9)$$

The second term, $\Delta P = (-16\pi N^2/3V^2)(\epsilon\sigma^6/r_c^3)$, represents the cutoff correction for the pressure in analogy to equation (A.5) for the energy. This is negative, which means that after taking the correction into account, we find that the simulation actually has been performed at a lower pressure than P_0. The volume change necessary to compensate for that and get back to the pressure P_0 is negative and can be estimated by inserting the pressure change ΔP into a discretized version of the compressibility definition $\Delta V = \kappa V \Delta P$, leading to

$$\Delta V = -\kappa \frac{16\pi N^2}{3V} \frac{\epsilon \sigma^6}{r_c^3}. \qquad (A.10)$$

REFERENCES

Alper, H. E., D. Bassolino, and T. R. Stouch. 1993a. Computer simulation of a phospholipid monolayer-water system: the influence of long range forces on water structure and dynamics. J. Chem. Phys. 98:9798–9807.

Alper, H. E., D. Bassolino-Klimas, and T. R. Stouch. 1993b. The limiting behavior of water hydrating a phospholipid monolayer: a computer simulation study. J. Chem. Phys. 99:5547–5559.

Bassolino-Klimas, D., H. E. Alper, and T. R. Stouch. 1993. Solute diffusion in lipid bilayer-membranes: an atomic level study by molecular dynamics simulation. Biochemistry. 32:12624–12637.

Berendsen, J. H. C., B. Egberts, S.-J. Marrink, and P. Ahlstrom. 1992. Molecular dynamics simulations of phospholipid membranes and their interaction with phopholipase A₂. In Membrane Proteins: Structures, Interactions and Models. A. Pullman, J. Jortner, and B. Pullman, editors. Kluwer Academic Publishers, Dordrecht, the Netherlands. 457–470.

Berendsen, J. H. C., J. P. M. Postma, W. F. van Gunsteren, A. DiNola, and J. R. Haak. 1984. Molecular dynamics with coupling to an external bath. J. Chem. Phys. 81:3684–3690.

Brooks, B. R., R. E. Bruccoleri, B. D. Olafson, D. J. States, S. Swaminathan, and M. Karplus. 1983. CHARMM: a program for macromolecular energy minimization and dynamics calculation. J. Comp. Chem. 4:187–217.

Büldt, G., H. U. Gally, J. Seelig, and G. Zaccai. 1979. Neutron diffraction studies on phosphatidylcholine model membranes. J. Mol. Biol. 134: 673–691.

Chiu, S., M. Clark, V. Balaji, S. Subramaniam, H. Scott, and E. Jakobsson. 1995. Incorporation of surface tension into molecular dynamics simula-

tion of an interphase: a fluid phase lipid bilayer membrane. Biophys. J. 69:1230–1245.

Damodaran, K. V., and K. M. Merz. 1994. A comparison of DMPC- and DLPE-based lipid bilayers. Langmuir. 9:1179–1183.

De Young, L. R., and K. A. Dill. 1988. Solute partitioning into lipid bilayer membranes. Biochemistry. 27:5281–5289.

Egberts, E., S. J. Marrink, and H. J. C. Berendsen. 1994. Molecular dynamics simulation of a phospholipid membrane. Eur. Biophys. J. 22:423–436.

Essex, J., M. Hann, and W. Richards. 1994. Molecular dynamics simulation of a hydrated phospholipid bilayer. Phil. Trans. R. Soc. Lond. B. 344:239–260.

Feller, S. E., Y. Zhang, and R. W. Pastor. 1995. Computer simulation of liquid/liquid interfaces. II. Surface tension-area dependence of a bilayer and monolayer. J. Chem. Phys. 103:10267–10276.

Franks, N. P. 1977. Structural analysis of hydrated egg lecithin and cholesterol bilayers. I. X-ray diffraction. J. Mol. Biol. 100:345–358.

Gawrisch, K., D. Ruston, J. Zimmerberg, V. Parsegian, R. Rand, and N. Fuller. 1992. Membrane dipole potentials, hydration forces, and the ordering of water at membrane surfaces. Biophys. J. 61:1213–1223.

Heller, H., M. Schaefer, and K. Schulten. 1993. Molecular dynamics simulation of a bilayer of 200 lipids in the gel and in the liquid-crystal phases. J. Phys. Chem. 97:8343–8360.

Huang, P., J. J. Perez, and G. H. Low. 1994. Molecular dynamics simulations of phospholipid bilayers. J. Biomol. Struct. Dyn. 11:927–956.

Jähnig, F. 1996. What is the surface tension of a lipid bilayer? Biophys. J. 71:1348–1349.

Jorgensen, W., J. Madura, and C. Swenson. 1984. Optimized intermolecular potential functions for liquid hydrocarbons. J. Am. Chem. Soc. 106:6638–6646.

Jorgensen, W., and J. Tirado-Rives. 1988. The OPLS potential functions for proteins. Energy minimizations for crystals of cyclic peptides and crambin. J. Am. Chem. Soc. 110:1657–1666.

Landau, L., and E. Lifschitz. 1938. Statistical Physics. Oxford University Press.

Lewis, B. A., and D. M. Engelman. 1983. Lipid bilayer thickness varies linearly with acyl chain length in fluid phosphatidylcholine vesicles. J. Mol. Biol. 166:211–217.

Marrink, S. J., M. Berkowitz, and H. J. C. Berendsen. 1993. Molecular dynamics simulation of a membrane/water interface: the ordering of water and its relation to the hydration force. Langmuir. 9:3122–3131.

Nagle, J. F. 1993. Area/lipid of bilayers from NMR. Biophys. J. 64: 1476–1481.

Nagle, J. F., and M. C. Wiener. 1988. Structure of fully hydrated bilayer dispersions. Biochim. Biophys. Acta. 942:1–10.

Peters, G. H., S. Toxvaerd, A. Svendson, and H. Olsen. 1994. Modeling of complex biological systems. I. Molecular dynamics studies of diglyceride monolayers. J. Chem. Phys. 100:5996–6010.

Raghavan, M., M. R. Reddy, and M. L. Berkowitz. 1992. A molecular dynamics study of the structure and dynamics of water between dilauroylphosphatidylethanolamine bilayers. Langmuir. 8:233–240.

Rand, R., and V. Parsegian. 1989. Hydration forces between phospholipid bilayers. Biochim. Biophys. Acta. 988:351–376.

Robinson, A., W. Richards, P. Thomas, and M. Hann. 1994. Head group and chain behaviour in biological membranes: a molecular dynamics study. Biophys. J. 67:2345–2354.

Rowlinson, J. S., and B. Widom. 1982. Molecular Theory of Capillarity. Oxford University Press.

Ryckaert, J. P., and A. Bellemans. 1975. Molecular dynamics of liquid n-butane near its boiling point. Chem. Phys. Lett. 30:123–125.

Ryckaert, J. P., and A. Bellemans. 1978. Molecular dynamics of liquid alkanes. Faraday Discuss. Chem. Soc. 66:95–106.

Seelig, J., and A. Seelig. 1974. Dynamic structure of fatty acyl chains in a phospholipid bilayer measured by DMR. Biochemistry. 13:4839–4845.

Shinoda, W., T. Fukada, S. Okazaki, and I. Okada. 1995. Molecular dynamics simulation of the dipalmitoylphosphatidylcholine (DPPC)

lipid bilayer in the fluid phase using the Nose-Parrinello-Rahman NPT ensemble. *Chem. Phys. Lett.* 232:308–312.

Tieleman, D. P., and H. J. C. Berendsen. 1996. Molecular dynamics simulations of fully hydrated DPPC with different macroscopic boundary conditions and parameters. *J. Chem. Phys.* 105:4871–4879.

Toxvaerd, S. 1990. Molecular dynamics calculation of the equation of state of alkanes. *J. Chem. Phys.* 93:4290–4295.

Tu, K., D. Tobias, and M. Klein. 1995. Constant pressure and temperature molecular dynamics simulation of a fully hydrated liquid crystal phase dipalmitoylphosphatidylcholine. *Biophys. J.* 69:2558–2562.

van Buuren, A. R., S. J. Marrink, and H. J. C. Berendsen. 1993. A molecular dynamics study of the decane/water interface. *J. Phys. Chem.* 97:9206–9212.

van Gunsteren, W. F., and H. J. C. Berendsen. 1987. Groningen Molecular Simulation (GROMOS) Library Manual. Biomos, Nijenborgh 4, 9747 AG Groningen, the Netherlands.

Venable, R., Y. Zhang, B. Hardy, and R. Pastor. 1993. Molecular dynamics simulations of a lipid bilayer and of hexadecane: an investigation of membrane fluidity. *Science.* 262:223–226.

Weiner, S. J., P. A. Kollman, D. A. Case, U. C. Singh, C. Ghio, G. Alagona, S. Profeta, and P. Weiner. 1984. A new force field for molecular mechanical simulation of nucleic acids and proteins. *J. Am. Chem. Soc.* 106:765–784.

Zhou, F., and K. Schulten. 1995. Molecular dynamics study of a membrane water interface. *J. Phys. Chem.* 99:2194–2207.